Published in final edited form as:
Curr HIV Res. 2008 May ; 6(3): 218–229.

Transcytosis-Blocking Abs Elicited by an Oligomeric Immunogen Based on the Membrane Proximal Region of HIV-1 gp41 Target Non-Neutralizing Epitopes

Nobuyuki Matoba[1], **Tagan A. Griffin**[1], **Michele Mittman**[1], **Jeffrey D. Doran**[1], **Annette Alfsen**[2], **David C. Montefiori**[3], **Carl V. Hanson**[4], **Morgane Bomsel**[2], and **Tsafrir S. Mor**[1,*]

[1] Center for Infectious Diseases and Vaccinology, The Biodesign Institute and School of Life Sciences, Arizona State University, Tempe, AZ, USA

[2] Department de Biologie Cellulaire, Institut Cochin. 22, rue Méchain, Paris, France

[3] Laboratory for AIDS Vaccine Research & Development Department of Surgery, Duke University Medical Center, Durham, NC, USA

[4] Viral and Rickettsial Disease Laboratory, California Department of Public Health, Richmond, CA, USA

Abstract

CTB-MPR$_{649–684}$, a translational fusion protein consisting of cholera toxin B subunit (CTB) and residues 649–684 of gp41 membrane proximal region (MPR), is a candidate vaccine aimed at blocking early steps of HIV-1 mucosal transmission. Bacterially produced CTB-MPR$_{649–684}$ was purified to homogeneity by two affinity chromatography steps. Similar to gp41 and derivatives thereof, the MPR domain can specifically and reversibly self-associate. The affinities of the broadly-neutralizing monoclonal Abs 4E10 and 2F5 to CTB-MPR$_{649–684}$ were equivalent to their nanomolar affinities toward an MPR peptide. The fusion protein's affinity to GM1 ganglioside was comparable to that of native CTB. Rabbits immunized with CTB-MPR$_{649–684}$ raised only a modest level of anti-MPR$_{649–684}$ Abs. However, a prime-boost immunization with CTB-MPR$_{649–684}$ and a second MPR$_{649–684}$-based immunogen elicited a more productive anti-MPR$_{649–684}$ antibody response. These Abs strongly blocked the epithelial transcytosis of a primary subtype B HIV-1 isolate in a human tight epithelial model, expanding our previously reported results using a clade D virus. The Abs recognized epitopes at the N-terminal portion of the MPR peptide, away from the 2F5 and 4E10 epitopes and were not effective in neutralizing infection of CD4+ cells. These results indicate distinct vulnerabilities of two separate interactions of HIV-1 with human cells – Abs against the C-terminal portion of the MPR can neutralize CD4+-dependent infection, while Abs targeting the MPR's N-terminal portion can effectively block galactosyl ceramide dependent transcytosis. We propose that Abs induced by MPR$_{649–684}$-based immunogens may provide broad protective value independent of infection neutralization.

Keywords

HIV vaccine; mucosal transmission; functional non-neutralizing antibodies; prime/boost; transcytosis

*Address correspondence to this author at the Biodesign Institute and School of Life Sciences, P.O. Box 874501, Arizona State University, Tempe, AZ 85287-4501, USA; Tel: 480 727-7405; Fax: 480 727-7615; tsafrir.mor@asu.edu.

INTRODUCTION

The envelope proteins of HIV-1, gp41 and gp120, have been at the focus of intense research since the discovery of the virus as the causal agent of AIDS, research that unraveled the protein's pivotal roles in viral transmission and infection. Consequently both proteins, gp120 in particular, became attractive as targets for various post-exposure and prophylactic intervention strategies [1]. During the last couple of years, in light of major impasses in clinical trials with several monomeric gp120-based vaccine candidates, gp41 has been gaining increasing attention as a new vaccine target, with a principal focus upon its highly conserved membrane proximal region (MPR) ectodomain, which contains the epitopes of the broadly neutralizing monoclonal Abs (mAbs) 2F5 and 4E10. It was suggested that these epitopes are linear [2–5] and several candidate vaccines were designed in the hope of inducing 2F5- or 4E10-like neutralizing Abs, but such efforts have been unsuccessful to date (reviewed in: [6]).

More recently the gp41 MPR was shown to play a central role in proposed non-fusogenic mechanisms of HIV-1 mucosal transmission such as transcytosis. Specifically, MPR binds to the glycosphingolipid galactosylceramide (GalCer) and the heparan sulfate proteoglycan agrin on the apical surface of epithelial cells, thereby triggering transcytosis of the virus towards the serosal side [7,8]. In fact, MPR-specific Abs such as 2F5 or, importantly, secretory IgAs present in mucosal secretions of highly exposed persistently negative individuals, were demonstrated to efficiently block transcytosis [9–14]. The GalCer binding site was shown to encompass the MPR residues 649–684 ($MPR_{649–684}$) [7]. Based on these findings, we have previously constructed CTB-$MPR_{649–684}$, a translational fusion protein comprising the non-toxic mucosal adjuvant cholera toxin B subunit (CTB) and $MPR_{649–684}$, as a vaccine candidate aimed at blocking the viral transmission pathway. The protein has been successfully shown to induce transcytosis-blocking anti-MPR Abs (serum IgG and secreted IgA) in mice following a heterologous route prime-boost immunization regimen [15,16].

Because mouse antisera are considered unreliable in neutralization studies it was important to test the immunogenicity of CTB-$MPR_{649–684}$ in a second animal model, e.g. rabbits. To this end, we established a purification procedure to isolate uniform CTB-$MPR_{649–684}$ pentamers and analyzed the purified protein's antigenic and functional domains. We then immunized rabbits with the immunogen and examined the antiviral activities of $MPR_{649–684}$-specific Abs thus obtained.

MATERIAL AND METHODS

Expression in Escherichia coli and purification of CTB-$MPR_{649–684}$

CTB-$MPR_{649–684}$ was expressed in *E. coli* and purified as previously described [16] with modifications. Briefly, late log-phase bacteria (OD_{500}=0.8–1.0) were induced by adding 0.3 mM isopropyl-1-thio-L-D-galactopy-ranoside (IPTG) to the medium followed by a further 2-h incubation period under growth conditions, after which the cells were harvested, resuspended (PBS + 1 mM phenylmethylsulphonyl fluoride) and homogenized by a French press (2 × 18,000 psi). The insoluble pellet obtained following centrifugation (30,000 × g for 15 min) was resuspended in TALON buffer (20 mM Tris, pH 8.0, 0.5 M NaCl) supplemented with 1.5% (m/v) 3-[(3-Cholamidopropyl)di-methylammonio]-1-propanesulfonate (CHAPS, Pierce), sonicated briefly, incubated on ice for 30 min with gentle agitation and centrifuged as described above. The CHAPS-solubilized fraction containing CTB-$MPR_{649–684}$ was filtered through a 0.45 μm filter, and was applied to a cobalt-charged agarose resin (TALON, BD Clontech). Purification generally followed manufacturer's instructions, with the addition of 0.5% (m/v) CHAPS in all solutions. The resin-bound CTB-$MPR_{649–684}$ was then eluted with 150 mM imidazole in TALON-CHAPS buffer and the eluate was directly applied to an immobilized D-

galactose resin (PIERCE) equilibrated with galactose binding buffer (50 mM Tris, pH 8.0, 0.5% CHAPS, 0.2 M NaCl, 5 mM D-galactose). The column was washed with galactose binding-buffer, then with galactose wash buffer (50 mM Tris, pH 8.0, 0.5% CHAPS, 0.5 M NaCl, 20 mM D-galactose), and eluted with galactose elution buffer (20 mM Tris, pH 8.0, 0.5% CHAPS, 0.5 M NaCl, 1 M D-galactose). The eluate was extensively dialyzed against PBS, pH 7.2, and the protein pellet formed under these conditions (see text) was collected by brief centrifugation, further washed with PBS, and stored at −80°C until use.

SDS-PAGE and immuno-blotting

SDS-PAGE and non-denaturing PAGE were conducted as previously described [16]. After electrophoresis, gels were stained, or proteins were electro-transferred to a poly (vinylidene difluoride) membrane. Blots were probed with either goat anti-CTB antiserum (1:10,000, List Biological Laboratories, Campbell, CA) followed by horseradish peroxidase (HRP)-conjugated rabbit anti-goat (1:20,000, Sigma), or by human mAb 2F5 (100 ng/mL) followed by HRP-conjugated goat anti-human (1:10,000, Calbiochem) Abs. Abs were detected using chemiluminscence (Santa Cruz).

Amino acid sequence analysis and mass spectrometry

The N-terminal sequence of recombinant CTB-$MPR_{649–684}$ was determined using a Procise 492 Protein Sequencer (Applied Biosystems), whereas molecular mass of the protein was analyzed by matrix assisted laser desorption/ionization time-of-flight mass spectrometry (Voyager-DE STR, MALDI-TOF mass spectrometer, Applied Biosystems).

Immunization

Three female New Zealand White rabbits were subcutaneously immunized with 25 μg of CTB-$MPR_{649–684}$ conjugated with liposome (pre-Liposome Formulation 2, Sigma) at week 0, 1 and 3, and boosted with 100 μg of the immunogen at week 7. Serum IgG levels were determined by ELISA as described above, using peroxidase-conjugated anti-rabbit IgG (Santa Cruz). For prime-boost experiments, three additional rabbits were primed with $MPR_{649–683}$ peptide chemically linked to keyhole limpet hemocyanin (KLH, Pierce Biotechnology) which was conjugated with Freund's complete adjuvant (87.5 μg per rabbit as KLH basis) at week 0, and then boosted with 25 μg of CTB-$MPR_{649–684}$ conjugated with liposome at week 19 and 36.

ELISA

In all ELISA analyses, 96 well polystyrene plates (ScreenMates, Matrix Technologies) were coated with 50 μL/well of samples dissolved in coating buffer (15 mM Na_2CO_3, 19 mM $NaHCO_3$, 3 mM NaN_3, pH 9.6), incubated for 1h at 37°C, and then blocked with 5% non-fat dry milk in PBS, pH 7.2, containing 0.05% (v/v) Tween-20 (PBST) for 1h at room temperature. Samples to analyze, and primary and HRP-conjugated secondary Abs were diluted in 1% non-fat dry milk in PBST, and incubated on plates for 1h at 37°C (50 μL/well). Specific binding was then detected with Sigma FAST OPD (ophenylenediamine dihydrochloride) substrate (Sigma) and quantitated by reading the absorbance at 490nm using a plate reader (SpectraMax 340PC, Molecular Devices). For the assays based on streptavidin-biotin interaction, bovine serum albumin (Sigma) was used in place of non-fat dry milk for blocking and sample preparation to maximize assay sensitivity.

To determine the apparent affinities of 2F5 and 4E10 mAbs to the MPR in various contexts, plates were coated with 5 μg/mL of streptavidin (Calbiochem) or 2 μg/mL of GM1 ganglioside (monosialoganglioside GM1, Sigma), which were then overlaid with the indicated concentrations of biotinylated peptides or CTB-$MPR_{649–684}$ (respectively). The mAbs (0.5

μg/mL) then reacted with the captured antigens, followed by detection with HRP-conjugated anti-human IgG (Calbiochem) at a 1:2000 dilution.

To compare the apparent affinities of CTB and CTB-$MPR_{649–684}$ to GM1 ganglioside, 96-plates were coated with 2 μg/mL GM1 gangliosides (Sigma), overlaid with a solution of biotinylated CTB (0.2 μM, List Biological Lab) and CTB (List Biological Lab) or CTB-$MPR_{649–684}$ (concentration range 0–2 μM). ELISA was developed using streptavidin-HRP (Calbiochem) and Sigma FAST OPD, and A490 was measured.

For rough epitope mapping, plates were coated with streptavidin as above. Then, one of four biotinylated peptides, $MPR_{649–684}$, $MPR_{649–662}$ (N-terminus), $MPR_{659–677}$ (core) or $MPR_{671–684}$ (C-terminus) was added to the wells. The peptides were added at a concentration of 1 μM. After incubation at 37°C for 1h, 2-fold serially diluted IgG samples starting at 10 μg/mL (purified from immunized rabbit sera using Protein A, Pierce) were added to the wells. After 1hr incubation at 37°C, the plates were washed and HRP-conjugated goat anti-rabbit IgG (Santa Cruz) was added to the wells at 1:3000 dilution and developed as above.

Binding parameters

Data obtained through competition experiments were fitted by nonlinear regression using GraphPad Prism 4.0 in order to obtain Kd or IC50 (respectively). Synthetic peptides were synthesized on a PerSeptive Biosystems 9050 synthesizer at Arizona State University's Protein Chemistry Laboratory.

Co-precipitation assay

Biotinylated $MPR_{649–684}$ peptide (300 μM in PBS, pH 7.4) was mixed with equal volumes of either CTB-$MPR_{649–684}$ or native CTB (4 μM in PBS, pH 7.4, containing 0.5% CHAPS) and then dialyzed (10 KD cut-off membrane) against PBS overnight at 4 °C to remove the detergent. Samples were then collected from the dialysis tube and centrifuged at 12,000 × g for 10 min. Supernatant was carefully removed, and the pellets were washed 2 × with PBS and analyzed by SDS-PAGE and Western blotting using anti-CTB or 2F5 as described above.

Pull-down assay

CTB-$MPR_{649–684}$ or native CTB at a concentration of 0.6 μM in PBS were mixed with 40 μM of biotinylated $MPR_{649–684}$ peptide in a volume of 1 mL and incubated overnight at 4 °C. CTB-$MPR_{649–684}$ stays soluble under these conditions. Samples were then centrifuged at 17,000× g for 10 min to remove any precipitate. Streptavidin-conjugated beads (PIERCE) were then added and allowed to form complexes with biotinylated $MPR_{649–684}$ for 1 h at room temperature. Beads were thoroughly washed with PBS containing 0.05% (v/v) Tween-20 and analyzed by SDS-PAGE and immuno- blotting using anti-CTB or 2F5 as described above.

Hemagglutination assay

A 10% suspension of washed sheep erythrocytes (Innovative Research) was fixed with an equal volume of 0.5% (v/v) glutaraldehyde solution in PBS. After incubation at 37 °C for 30 min, the cells were spun down at 1,000× g for 1 min. The cells were then washed and resuspended at a concentration of 5% in PBS. To remove residual aldehyde groups, 50 mM of glycine was added and the pH was adjusted to 11. The cells were incubated at 4 °C overnight with gentle shaking. The erythrocytes were then spun down and resuspended to 10% in 0.1N NaOH solution containing 250 μM GM1 gangliosides. After 6 h incubation at 45 °C, the cells were washed in PBS, and resuspended to 1% in PBS containing 3 g/L BSA and 1 g/L sodium azide. Serial dilutions of CTB or CTB-$MPR_{649–684}$ in PBS were mixed with an equal volume of GM1

ganglioside-coated erythrocytes in a 96-well round bottom plate and incubated overnight at 4 °C.

Hydropathy analyses

Peptide hydrophobicity was analyzed using the scale of Kyte and Doolittle [17], whereas hydrophilicity was plotted using the algorithm of Hopp and Woods [18] (www.expasy.ch/cgi-bin/protscale.pl). The average values of each seven-amino acid fragment of peptides were plotted along the sequence.

Single-round pseudovirus infection reporter gene assay

The assay was conducted as described previously [19]. Clade B pseudotyped viruses were produced in H9 (for MN) or 293T cells (for SF162.LS, WITO4160.33, REJO4541.67, SC422661.8). Briefly, pseudovirus at a concentration equivalent to 200x tissue culture infectious dose 50 ($TCID_{50}$) was mixed with purified IgG samples and incubated for 1 h at 37° C. The virus-serum mixture was then added to the plated TZM-bl cells, and cultured for additional 48 h. Cells were lysed, and luciferase activity of each well was measured. The 50% inhibitory concentration (IC_{50}) was calculated as the sample concentration that caused a 50% reduction in relative luminescence units (RLU) compared to the virus control after subtraction of luminescence in cell controls.

Peripheral blood mononuclear cell (PBMC) assay

The assay was conducted essentially as previously described [20]. Human PBMCs were prepared from buffy coats provided by a local blood bank, using LSM Lymphocyte Separation Medium (Cappel). Briefly, 0.1 mL culture medium containing HIV-1 at a concentration of 100x $TCID_{50}$ was mixed in quadruplicate with 0.1 mL of serial twofold dilutions of IgG samples and incubated for 1 h at 37°C. The mixture was then incubated with 250,000 of phytohemagglutinin-stimulated PBMC in 0.05 ml per well. After 3 days the cells were washed extensively, and cultured for 1 additional day, at which time viral expression was assayed by a commercially available p24 ELISA (Beckman-Coulter; Fullerton, CA). Neutralization was defined as the percent reduction in the amount of p24 detected from wells treated with the test samples as compared with control wells. For comparison purposes, the concentration of the test agent required for 50, 90 and 100% neutralization was determined *via* linear regression analysis using the SoftMax Pro software (Molecular Devices). Heat-inactivated, human HIV-1-neutralizing plasma was used as a positive control [21,22].

Transcytosis assay

The assay was performed using human epithelial cell lines (intestinal carcinoma HT29 clone 19 or endometrial cell line HEC-1) and human peripheral blood mononuclear cells infected with HIV-1 clade B R5 tropic 92BR029 (NIH AIDS Research and Reference Reagent Program) as previously described [16,23]. Protein A-purified rabbit IgG samples were dialyzed against PRMI 1640 with 10% fetal calf serum, and tested. For analysis of the MPR reversion of the neutralizing activity, samples were incubated overnight at 4°C with 50 μg/mL of biotinylated $MPR_{649–684}$ peptide. The MPR-bound Abs were then removed by precipitation with streptavidin sepharose. As a negative control, IgGs from untreated rabbits were used. Results are expressed as percent of transcytosis observed with the corresponding samples obtained from untreated control rabbits. Experiments were repeated at least twice for all conditions with each of the two cell types and results shown reflect the mean of at least 4 repeats.

Statistical Analysis

Statistical analysis was conducted by using GraphPad Prism 4 software. The repeated-measures ANOVA followed by Bonferroni's multiple comparison test was used to compare the level of

anti-MPR Abs to the one at Week 0 for immunized rabbits in Fig. 5A. A p-value < 0.05 was taken as significant.

RESULTS

Purification of CTB-MPR$_{649–684}$ expressed in E. coli

Immuno-blot analysis revealed two protein bands that were reactive to anti-CTB and 2F5 Abs in cell extracts of IPTG-induced bacteria (Fig. 1A–C). Of these, the major protein had an apparent molecular mass that corresponded well to the calculated size of CTB-MPR$_{649–684}$ (17.7 kDa) while the minor band had a higher apparent molecular mass (20 kDa), consistent with that of unprocessed CTB-MPR$_{649–684}$ (i.e. retaining the pelB periplasm-targeting signal). The *E. coli* signal peptidase is situated at the periplasmic face of the plasma membrane [24]. Therefore, the apparent processing of CTB-MPR$_{649–684}$ suggests that the fusion protein accumulates within the periplasmic space. Based on a densitometric image analysis, the amount of putatively processed CTB-MPR$_{649–684}$ was estimated to be approximately 8% of the total *E. coli* protein. Incubation in the presence of the inducer for more than 2 h did not result in higher levels of accumulation (data not shown).

We had previously used metal affinity chromatography to purify CTB-MPR$_{649–684}$ [16]. While this protocol yielded sufficient purity (>99%), the resultant protein preparation consisted of both correctly assembled pentameric CTB-MPR$_{649–684}$ and misfolded, mostly monomeric fusion protein. To overcome this limitation, we developed an improved purification method. Interestingly, the majority of expressed CTB-MPR$_{649–684}$ was found in the insoluble fraction after disrupting cells in PBS, despite the apparent successful localization within the periplasmic space (Fig. 1A). Previously, we used sub-denaturing concentrations of urea to solubilize CTB-MPR$_{649–684}$. However, we found that the zwitterionic detergent CHAPS can solubilize the putatively processed protein more efficiently than urea (Fig. 1A–C, lane 5). Following solubilization with CHAPS, CTB-MPR$_{649–684}$ was purified by in-tandem affinity chromatography: first, cobalt affinity TALON resin was used to specifically enrich the histidine-tagged fusion protein; second, an immobilized galactose resin was used to selectively bind pentameric CTB-MPR$_{649–684}$ [25,26]. We found that TALON resin is advantageous over conventional nickel resins because the former requires less imidazole (150 mM *vs* 1 M were needed) to elute the histidine-tagged CTB-MPR$_{649–684}$, allowing the TALON eluate to be directly applied onto the following galactose affinity resin without any additional treatments such as dialysis or desalting. As shown in Fig. 1A, the resultant CTB-MPR$_{649–684}$ purified with this procedure appears virtually pure on a SDS-PAGE gel. Electrophoresis under non-denaturing conditions showed that a majority of the metal affinity-purified CTB-MPR$_{649–684}$ was organized into pentamers, and a trace amount of monomers in the metal affinity fraction had been successfully eliminated by the subsequent galactose affinity purification step, yielding substantially uniform pentamers (Fig. 1D). The molecular mass of the purified protein was determined by mass-spectrometry to be 17,745 Da, corresponding well (0.021% deviation) with the predicted molecular mass, 17,749 Da, of the pelB-cleaved form (Fig. 1E). Generation of the mature N-terminus was further confirmed by N-terminal sequencing, revealing that the 22 amino-acid pelB signal-peptide was successfully cleaved. Using this protocol we were able to consistently obtain more than 0.5 mg of pure CTB-MPR$_{649–684}$ from 1 liter of culture representing a typical yield of 50%.

Affinity of the broadly neutralizing gp41 mAbs to CTB-MPR$_{649–684}$.

Both the gp41-specific mAbs 2F5 and 4E10 are broadly neutralizing. Of the two, however, 2F5 rarely neutralizes clade C viruses, the most common in Sub-Saharan Africa [27–29]. We have previously demonstrated that CTB-MPR$_{649–684}$ can be recognized by 2F5 [16]. Because the protein also harbors the 4E10 epitope, it was imperative to demonstrate the binding of 4E10,

and further assess the relative affinities of the two mAbs to the fusion protein as compared to the free peptide. To this end, we have used a modified ELISA assay employing, as controls, two synthetic N-terminally biotinylated peptides: $bMPR_{649–683}$ (biotin-SQT QQEKNEQELLELDK-WASLWNWFDITNWLWYIK) and $bMPR_{659–677}$ (biotin-ELLELDKWASLWNWFDIT), a shorter MPR peptide consisting of core epitopes of the two mAbs. In order to increase the potential for the peptides to interact with the immunoglobulin, we used streptavidin pre-adsorbed to the plates to capture the peptides. CTB-$MPR_{649–684}$ was captured by GM1 gangliosides. In comparing the free peptide with the fusion proteins we took into account the molar concentration of the MPR moiety (i.e. 5 molecules of peptide are equivalent to 1 pentameric CTB-$MPR_{649–684}$). About the same number of MPR moieties per well were bound as evident by the roughly equal OD_{490} readings at saturation for all ligand/Ab combinations (except 4E10 and $bMPR_{659–677}$,Fig. 2). As shown in Fig. 2 and calculated in Table 1, the analysis revealed that both 2F5 and 4E10 recognized CTB-$MPR_{649–684}$, with low nano-molar affinities comparable to those of synthetic $MPR_{649–683}$ (2.0 nM *vs* 1.7 nM for 2F5, and 2.6 nM *vs* 6.9 nM for 4E10, respectively), indicating that the fusion protein in its receptor-binding form presents antigenically competent MPR. Interestingly, 4E10 exhibited substantially lower affinity to $MPR_{659–677}$ than those to $MPR_{649–683}$ or CTB-$MPR_{649–683}$ (K_d= ~50 nM) although the $MPR_{659–677}$ sequence spans the reported epitope for this mAb [2]. This suggests that additional residues of the MPR may coordinate the binding of 4E10 [5,30].

Specific molecular associations of CTB-$MPR_{649–684}$

We found that at concentrations >1 μM, CTB-$MPR_{649–684}$ gradually forms precipitate upon removal of the detergent by dialysis against PBS at pH 7.2. This is in sharp contrast to native CTB, which was completely soluble in the same buffer at greater than 30 μM. The precipitation of CTB-$MPR_{649–684}$ appeared to be pH dependent; in higher pH solutions, solubility of CTB-MPR was greater, with complete solubilization obtained at pH 10 and higher. Since the only difference between the fusion protein and its native counterpart lies in the 35 amino-acid long $MPR_{649–684}$, we surmised that it is this gp41-derived peptide that is responsible for the relative lower solubility of CTB-$MPR_{649–684}$ as compared to its native counterpart. The reduced solubility could be a result of increased hydrophobicity of the fusion protein, or specific association between the $MPR_{649–684}$ domains. Indeed, the corresponding region of gp41 is generally rich in hydrophobic residues especially within its C-terminal region, even outside of the transmembrane domain (see below, Kyte & Doolittle plot in Fig. 7A). It should be noted, however, that free $MPR_{649–684}$ peptide is soluble even at 3 mM in PBS at pH7.4 (data not shown). Meanwhile, studies have shown that gp41-derived peptides have a tendency to reversibly associate into high order multimers [31–42]. In order to definitively distinguish between the two explanations, we incubated synthetic $bMPR_{649–683}$ peptides with either CHAPS-solubilized CTB-$MPR_{649–684}$ or with CTB, removed the detergent by extensive dialysis, and subjected the resulting precipitate to SDS-PAGE and immuno-blot analyses (Fig. 3A). While CTB-$MPR_{649–684}$ co-precipitated with the peptide, native CTB did not, indicating that the free peptide associates specifically with its fused counterpart. CTB-$MPR_{649–684}$ did not co-precipitate with a shorter MPR peptide, $bMPR_{659–677}$ (data not shown). To further demonstrate the specific association among the $MPR_{649–684}$ domains, a pull-down assay was performed. CTB-$MPR_{649–684}$ (soluble without detergent at the applied 0.6 μM concentration) or CTB were incubated with the biotinylated-peptide, which allowed for binding \ streptavidin-conjugated beads through the biotin moiety on the peptide prior to centrifugation and SDS-PAGE/immunoblot analyses. As shown in Fig. 3B, the assay demonstrated that CTB-$MPR_{649–684}$, but not native CTB, was co-fractionated with the streptavidin-$bMPR_{649–683}$ complex. Taken together, these results strongly argue in favor of the hypothesis that, like gp41 and its derivatives, the $MPR_{649–684}$ domains of the fusion protein are capable of specific

interactions with either the free peptide or with each other, leading to the formation of higher-order multimers of CTB-$MPR_{649–684}$ with diminished solubility.

Thus, the $MPR_{649–684}$ domain of the fusion protein appears to retain much of its biochemical identity. Our next goal was to determine if this is also true for the CTB fusion partner. Previously, we demonstrated that CTB-MPR can bind to GM1 gangliosides, like native CTB. However, because GM1-binding is considered to be crucial for mucosal targeting of the fusion protein, it is important to determine the GM1-binding affinities of CTB-$MPR_{649–684}$ as compared to CTB in order to evaluate whether the C-terminal fusion of the $MPR_{649–684}$ peptide to CTB has compromised its GM1 binding potency. To this end, we performed a hemagglutination assay using GM1-coated sheep red blood cells (Fig. 4A). Both CTB-$MPR_{649–684}$ and CTB exhibited clear hemagglutination activity starting at low nanomolar concentrations. This hemagglutination was a GM1-specific event because neither of the tested proteins showed such an effect on untreated cells (data not shown). Interestingly, however, we reproducibly observed that the concentration of CTB-MPR required for hemagglutination initiated was 2–4 fold lower than that of CTB. This may be explained by the self-association of MPR domains, as demonstrated above, bringing about inter-molecular bridging of CTB-$MPR_{649–684}$, which in turn resulted in the augmention of the hemagglutination effect provided by GM1-binding of the CTB domain. To assay the affinity of CTB-MPR to GM1 more directly, we performed a competitive GM1-ELISA. We included a detergent in the assay to avoid the self-association among the MPR domains that may affect the apparent GM1 affinities. As shown in Fig. 4B, CTB-$MPR_{649–684}$ bound to GM1 ganglioside in a concentration-dependent manner with low-nanomolar affinity (IC_{50} = 9.6 nM), which was essentially comparable to that of CTB (IC_{50} = 12.6 nM). These results demonstrate that the C-terminal MPR domains of the fusion protein do not interfere with the GM1-binding activity of the CTB domain and substantiate the notion that the $MPR_{649–684}$ domains are free to interact.

Antiviral effects of rabbit anti-$MPR_{649–684}$ Abs

Previously, we immunized mice with CTB-$MPR_{649–684}$ using heterologous route prime-boost regimen, which successfully induced robust mucosal and serum anti-MPR Abs with strong transcytosis-blocking activity directed against NDK, a clade D HIV-1 primary isolate [15, 16]. In this report, we turned to test the immunogenicity of the fusion protein in rabbits as a second animal model. Rabbits were able to elicit anti-MPR serum IgGs with an average endpoint titer of ~200 after three subcutaneous immunizations (Fig. 5A). Interestingly, subsequent booster immunizations with CTB-$MPR_{649–684}$ did not result in further augmentation of the anti-MPR Ab response (Fig. 5A), although anti-CTB Abs continued to increase with endpoint titers exceeding 100,000 (data not shown). These contrasting responses to the carrier in comparison to the hapten led us to postulate that the immunodominance of the former may be responsible. To examine this possibility, we immunized rabbits with a synthetic $MPR_{649–683}$ peptide that was chemically conjugated to key-hole limpet hemocyanin (KLH:$MPR_{649–683}$) and subsequently boosted them with CTB-$MPR_{649–684}$. Compared with a modest anti-MPR response in rabbits primed with the KLH:$MPR_{649–683}$ conjugate, the animals developed a more productive anti-MPR response following boosting with CTB-$MPR_{649–684}$ (Fig. 5B). Similarly, rabbits that were primed with CTB-$MPR_{649–684}$ and then boosted with KLH:$MPR_{649–683}$ also exhibited a sustained and enhanced anti-MPR response (data not shown). Therefore, the use of the two MPR-based immunogens in sequence (prime-boost regimen) yielded a stronger anti-MPR serum IgG response than CTB-$MPR_{649–684}$ alone. Interestingly, in a separate experiment, rabbits developed very limited mucosal anti-MPR IgA response following intranasal immunization or combination of intranasal and systemic (subcutaneous) immunizations in sharp contrast to our previously reported results in mice (Matoba and Mor, unpublished results).

The different quantitative outcome in mice and rabbits of the immunization raised the question of whether the two species are also different in the type of Abs elicited by the immunogens. We therefore tested serum-IgG enriched preparation obtained from the immunized rabbits (two animals that showed higher anti-$MPR_{649–683}$ IgG levels, i.e. No. 1 and 2 in Fig. 5B for antiviral activities. Transcytosis-blocking effects on a clade B R5 tropic virus (primary isolate 92BR029 from the NIH repository) were tested in the human tight epithelial model. As shown in Fig. 6, antibody samples effectively inhibited the transcytotic process, while the IgG sample from a control untreated rabbit did not (91–98% inhibition). Transcytosis-blocking effect was anti-MPR Abs specific, as depletion of these Abs by biotinylated-MPR peptide conjugated with streptavidin beads partially reversed the effect. The partial nature of the reversal, also observed in our earlier reports, could be due to the possibility that the polyclonal IgG preparation contains Abs directed at conformational epitopes present on the virus and not on the biotinylated-MPR peptide in solution.

In sharp contrast, the same antibody samples did not neutralize HIV-1 infection in the single-round pseudovirus infectivity assay (Table 2), or in a neutralization assay using human PBMCs (Table 3). These results reveal that although the MPR is targeted by the mAbs 2F5 and 4E10 as well as by the polyclonal Abs raised in our experiments, they exhibit different antiviral activities. This raises the possibility that the transcytosis blocking Abs bind to different epitopes within the MPR peptide. To test this possibility we examined the reactivity of the rabbit Abs with three overlapping fragment peptides of MPR, i.e. $MPR_{649–662}$, $MPR_{659–677}$ and $MPR_{671–684}$ (Fig. 7). The results revealed that the majority of the anti-MPR IgGs target the hydrophilic N-terminal region of MPR. This is consistent with the prediction by the Hopp-Woods analysis that the N-terminal region is more “antigenic” than the C-terminal region [18,43–45], while a marginal level of the IgGs were shown to recognize the hydrophobic C-terminal portion of the MPR that spans the 2F5 and 4E10 epitopes (Fig. 7). Thus, the region of the MPR critical for neutralization of CD4-dependent infection by Ab binding is demonstrated to be distinct from the region bound by non-neutralizing Abs elicited by CTB-$MPR_{649–684}$ that effectively block GalCer-dependent transcytosis: the former recognized epitopes concentrated close to the C-terminus of the MPR, while the latter Abs were preferentially reactive to the N-terminal half of the MPR. (This is in agreement with the structure of the MPR peptide as studied by NMR. See Coutant J, Yu HF, Alfsen A, Bomsel M, Toma F, and Curmi P. Structural flexibility of HIV gp41-membrane proximal region P1 peptide at physiological pH. XXIInd International Conference on Magnetic Resonance in Biological Systems (ICMRBS), Gottingen, Germany, August 2006).

DISCUSSION

The transmembrane envelope protein gp41 constitutes one of the most attractive targets in countermeasures to HIV-1 because of its pivotal roles in mucosal transmission and CD4+ cell infection. Our vaccine development strategy centers on the MPR of gp41 due to the pivotal role that the region plays in both membrane fusion and transcytosis processes [6,7]. We previously described the construction of a mucosally-targeted immunogen, CTB-$MPR_{649–684}$, and demonstrated its ability to induce transcytosis-blocking anti-MPR serum and mucosal Abs in mice. Here we describe detailed biochemical characterization of both the immunogen and the Abs induced in a second animal model, rabbits. Our results indicate that the $MPR_{649–684}$ moiety of the fusion protein can interact specifically with its counterparts on other CTB-$MPR_{649–684}$ molecules or the free MPR peptide, leading to creation of large assemblies. We further show that CTB-$MPR_{649–684}$ is immunogenic in rabbits and that the elicited Abs mostly recognize the N-terminal portion of the 35-amino acid peptide, away from the previously described epitopes of the neutralizing mAbs 2F5 and 4E10. While the rabbit Abs did not effectively inhibit infection of CD4+ cells in a pseudovirus assay or in a human PBMC neutralization assay, they exhibited effective transcytosis-blocking activity against a

B-clade HIV-1 primary isolate (in addition to the previously reported effects against a D-clade virus [15,16]).

In this study, we used a bacterial expression system and directed the recombinant protein to the periplasmic space to ensure proper processing, folding and pentamer assembly of CTB. While the majority of the recombinant protein was correctly localized (evident by the removal of the periplasmic targeting signal peptide), it was nonetheless insoluble and was recovered in the cell debris pellet following homogenization and fractionation. Although we cannot completely exclude the possibility that the protein was simply aggregated in inclusion bodies, the following evidence prompted us to hypothesize that the individual CTB-$MPR_{649–684}$ pentamers associate, rather than aggregate, into insoluble supramolecular complexes: 1) the protein could readily be made soluble by raising the pH to ~10 and using mild detergents (e.g. CHAPS, as used here, and *n*-dodecyl-β-D-maltoside, data not shown), and 2) substantial portion of the thus-solubilized protein was found to be correctly assembled into GM1-binding pentamers, an unlikely scenario if the protein was aggregated in inclusion bodies (Fig. 4A,B). Previous studies have shown that gp41 forms trimers, and its fragments also tend to associate into oligomers that are often less soluble at physiological pH [31–42]. We have substantiated our hypothesis that the association of CTB-$MPR_{649–684}$ into large complexes was a result of specific intra- as well as inter-molecule interactions among the MPR domains by demonstrating that CTB-$MPR_{649–684}$ could reversibly be taken in and out of solution and could be selectively co-precipitated with free MPR peptide (Fig. 3A). Moreover, a pull down assay confirmed these findings (Fig. 3B). Although at this point it is unclear how many MPR domains associate with each other (two, three, as in the viral envelope, or more), our findings lead us to propose, that the MPR domains of CTB-$MPR_{649–684}$ retain some of the conformational properties of the corresponding region within the context of native gp41. This may be a key factor in the success of this immunogen in inducing cross-clade transcytosis-blocking Abs (B sequence, effective against B and D clade viruses) in two animal models as demonstrated here and in our previous work.

Of interest is the fact that $MPR_{649–683}$ failed to form a complex with $MPR_{659–677}$ in co-precipitation and pull-down assays (data not shown). This suggests that the short fragment of MPR containing only 2F5 and 4E10 core epitopes (i.e. ELDKWA and NWFDIT) is not sufficient for the oligomerization of MPR, which probably requires the upstream stretch of amino acids contained in the N-terminal portion of the longer peptide. Interestingly, this region maps to the C-terminal heptad repeat of gp41 or HR2, and N-terminal extension of MPR to HR2 has been previously suggested to allow for oligomerization of MPR [31,46]. While the structure of the gp120 envelope protein was elucidated at atomic resolution [47], detailed structural data regarding gp41 in the pre-fusion state are scant especially for the intracellular, transmembrane and MPR domains [6]. Short peptides corresponding to the linear epitopes of 2F5 and 4E10 were co-crystallized with their respective mAbs and show a bent α-helical structure. However, as mentioned above, the structural features of the MPR are seemingly affected by the length of this domain. Further studies are required to elucidate the factor(s) involved in the oligomerization of MPR. Binding analyses with other gp41 constructs as well as physiochemical structure analyses may provide more insights.

GM1 ganglioside binding by CTB is considered to be crucial for its mucosal targeting and immunogenicity [48,49]. It is evident from the hemagglutination assay and competitive GM1-ELISA that CTB-$MPR_{649–684}$ preserves CTB's full capacity to bind GM1 gangliosides. Moreover, we demonstrated that pentameric CTB-$MPR_{649–684}$ retains its antigenicity to mAbs 2F5 and 4E10. Nonetheless, the anti-MPR Ab response in rabbits was weaker than the mice response we reported earlier [15,16], and unlike mice, could not be boosted by repeated immunization with CTB-$MPR_{649–684}$ (Fig. 5A). Considering that priming immunization alone resulted in high titers of Abs directed to the CTB domain and that these titers continued to rise

following the booster immunization, it seems reasonable to speculate that the humoral response to the MPR may have been overshadowed by the highly immunodominant CTB domain. The poor response to MPR does not appear to be a result of immunological tolerance, since we were able to recall a higher anti-MPR Ab response by a booster immunization with a second immunogen carrying the same MPR hapten (i.e. priming with KLH:$MPR_{649–683}$, boosting with CTB-$MPR_{649–684}$ (Fig. 5B). The species differences we observed could stem from the fact that the nasal associated lymphoid tissue of rabbit is rather different than that of rodents [50]. Although clearly not a clinical option in itself, the use of KLH:MPR nonetheless demonstrates that a prime boost approach of cross-immunization with different MPR-based immunogens may be a viable option to obtain a robust anti-MPR antibody response.

Similar to their murine counterparts [15,16], rabbit anti-MPR Abs successfully inhibited HIV-1 transcytosis in a human tight epithelial model (Fig. 6). Notably, the transcytosis-blocking effect was demonstrated for a CCR5 tropic, B clade primary isolate. This result confirms and expands our previous reports that show similar effects on another primary isolate of a clade D virus. Our results suggest that such anti-MPR Abs may be active against a broad spectrum of HIV-1 isolates, and this notion will be tested through comprehensive transcytosis assays.

The implied breadth of the antiviral activities of anti-MPR Abs that were elicited by our MPR-based immunogens was anticipated given the sequence conservation of the MPR across different HIV-1 subtypes, and the wide-ranging reactivity of the two gp41 neutralizing mAbs, that can efficiently block both infection of CD4+ cells and transcytosis. However, the same rabbit anti-MPR Abs that efficiently prevented transcytosis exhibited no neutralization of CD4-dependent infection in either the PBMC neutralization assay or the surrogate pseudovirus neutralization assay (Tables 2 and 3). These results clearly indicate that the inhibitory effects of anti-MPR Abs involve distinct mechanisms in the case of transcytosis and infection. This is congruent with these processes' reliance on a common co-receptor (CCR5) but on distinct primary receptors (GalCer and CD4, respectively) [51]. The epitope mapping of the transcytosis-blocking anti-$MPR_{649–684}$ Abs, even at the low resolution presented here, at once suggests a critical role of the N-terminal portion of $MPR_{649–684}$ in transcytosis (Fig. 7), and also ascribes an important anti-viral function to Abs targeting this region previously simply dismissed as "non-neutralizing, cluster-II-like" [6,52–54]. Furthermore, such Abs could act synergistically with peptides targeted at cross-linking activation receptors on phagocytic immune cells to effectively inhibit infection and replication of HIV in PBMC cultures (Eggink, Hanson, Salas, Matoba, Mor and Hoober, unpublished). Therefore, our results may support the important realization that Abs, with strong binding affinity to conserved regions of the HIV-1 envelope (thus capable of targeting virions to phagocytes [55,56]) may have a role to play in stopping mucosal transmission and infection of target cells, even if they lack "neutralization" capacity by themselves.

Acknowledgments

The authors gratefully acknowledge Maria Salas for her expert conductance of the PBMC assay and Jacquelyn Kilbourne for her excellent support in animal immunization. Work presented here was supported in part by NIH grants to TSM (IR21AI052761-01A2 and U19AI62150) and DCM (AI30034). NM acknowledges a JSPS Postdoctoral Fellowship for Research Abroad (awarded in 2004).

ABBREVIATIONS

Ab

Antibody

CHAPS

3-[(3-Cholamidopropyl)dimethylammonio]-1-propanesulfonate

CTB
Cholera toxin B subunit

GalCer
Galactosylceramide

HRP
Horseradish peroxidase

IPTG
Isopropyl-1-thio-L-D-galactopyranoside

KLH
Keyhole limpet hemocyanin

mAb
Monoclonal antibody

MPR
Membrane proximal region of gp41 (subscripted numbers refer to residue numbers in gp160, and the preceding lower case b indicates biotin-labeled peptides)

PBMC
Peripheral blood mononuclear cells

$TCID_{50}$
Tissue culture infectious dose 50

References

1. Zolla-Pazner S. Identifying epitopes of HIV-1 that induce protective antibodies. Nat Rev Immunol 2004;4:199–210. [PubMed: 15039757]
2. Zwick MB, Labrijn AF, Wang M, et al. Broadly neutralizing antibodies targeted to the membrane-proximal external region of human immunodeficiency virus type 1 glycoprotein gp41. J Virol 2001;75:10892–10905. [PubMed: 11602729]
3. Parker CE, Deterding LJ, Hager-Braun C, et al. Fine definition of the epitope on the gp41 glycoprotein of human immunodeficiency virus type 1 for the neutralizing monoclonal antibody 2F5. J Virol 2001;75:10906–10911. [PubMed: 11602730]
4. Muster T, Steindl F, Purtscher M, et al. A conserved neutralizing epitope on gp41 of human immunodeficiency virus type 1. J Virol 1993;67:6642–6647. [PubMed: 7692082]
5. Brunel FM, Zwick MB, Cardoso RM, et al. Structure-function analysis of the epitope for 4E10, a broadly neutralizing human immunodeficiency virus type 1 antibody. J Virol 2006;80:1680–1687. [PubMed: 16439525]
6. Zwick MB. The membrane-proximal external region of HIV-1 gp41: a vaccine target worth exploring. AIDS 2005;19:1725–1737. [PubMed: 16227780]
7. Alfsen A, Bomsel M. HIV-1 gp41 envelope residues 650–685 exposed on native virus act as a lectin to bind epithelial cell galactosyl ceramide. J Biol Chem 2002;8:8.
8. Alfsen A, Yu H, Magerus-Chatinet A, Schmitt A, Bomsel M. HIV-1-infected blood mononuclear cells form an integrin- and agrin-dependent viral synapse to induce efficient HIV-1 transcytosis across epithelial cell monolayer. Mol Biol Cell 2005;16(9):4267–79. [PubMed: 15975901]
9. Devito C, Hinkula J, Kaul R, et al. Cross-clade HIV-1-specific neutralizing IgA in mucosal and systemic compartments of HIV-1-exposed, persistently seronegative subjects. J Acquir Immune Defic Syndr 2002;30:413–420. [PubMed: 12138348]

10. Devito C, Broliden K, Kaul R, et al. Mucosal and plasma IgA from HIV-1-exposed uninfected individuals inhibit HIV-1 transcytosis across human epithelial cells. J Immunol 2000;165:5170–5176. [PubMed: 11046049]
11. Devito C, Hinkula J, Kaul R, et al. Mucosal and plasma IgA from HIV-exposed seronegative individuals neutralize a primary HIV-1 isolate. AIDS 2000;14:1917–1920. [PubMed: 10997395]
12. Broliden K, Hinkula J, Devito C, et al. Functional HIV-1 specific IgA antibodies in HIV-1 exposed, persistently IgG seronegative female sex workers. Immunol Lett 2001;79:29–36. [PubMed: 11595287]
13. Kaul R, Plummer F, Clerici M, Bomsel M, Lopalco L, Broliden K. Mucosal IgA in exposed, uninfected subjects: evidence for a role in protection against HIV infection. AIDS 2001;15:431–432. [PubMed: 11273233]
14. Belec L, Ghys PD, Hocini H, et al. Cervicovaginal secretory antibodies to human immunodeficiency virus type 1 (HIV-1) that block viral transcytosis through tight epithelial barriers in highly exposed HIV-1-seronegative African women. J Infect Dis 2001;184:1412–1422. [PubMed: 11709783]
15. Matoba N, Geyer BC, Kilbourne J, Alfsen A, Bomsel M, Mor TS. Humoral immune responses by prime-boost heterologous route immunizations with CTB-MPR(649–684), a mucosal subunit HIV/AIDS vaccine candidate. Vaccine 2006;24:5047–5055. [PubMed: 16621185]
16. Matoba N, Magerus A, Geyer BC, et al. A mucosally targeted subunit vaccine candidate eliciting HIV-1 transcytosis-blocking Abs. Proc Natl Acad Sci USA 2004;101:13584–13589. [PubMed: 15347807]
17. Kyte J, Doolittle RF. A simple method for displaying the hydropathic character of a protein. J Mol Biol 1982;157:105–132. [PubMed: 7108955]
18. Hopp TP, Woods KR. Prediction of protein antigenic determinants from amino acid sequences. Proc Natl Acad Sci USA 1981;78:3824–3828. [PubMed: 6167991]
19. Li M, Gao F, Mascola JR, et al. Human immunodeficiency virus type 1 env clones from acute and early subtype B infections for standardized assessments of vaccine-elicited neutralizing antibodies. J Virol 2005;79:10108–10125. [PubMed: 16051804]
20. D'Souza MP, Milman G, Bradac JA, McPhee D, Hanson CV, Hendry RM. Neutralization of primary HIV-1 isolates by anti-envelope monoclonal antibodies. AIDS 1995;9:867–874. [PubMed: 7576320]
21. Wang CY, Sawyer LS, Murthy KK, et al. Postexposure immunoprophylaxis of primary isolates by an antibody to HIV receptor complex. Proc Natl Acad Sci USA 1999;96:10367–10372. [PubMed: 10468614]
22. Wang CY, Shen M, Tam G, et al. Synthetic AIDS vaccine by targeting HIV receptor. Vaccine 2002;21:89–97. [PubMed: 12443666]
23. Bomsel M, Heyman M, Hocini H, et al. Intracellular neutralization of HIV transcytosis across tight epithelial barriers by anti-HIV envelope protein dIgA or IgM. Immunity 1998;9:277–287. [PubMed: 9729048]
24. Choi JH, Lee SY. Secretory and extracellular production of recombinant proteins using *Escherichia coli*. Appl Microbiol Biotechnol 2004;64:625–635. [PubMed: 14966662]
25. Yasuda Y, Matano K, Asai T, Tochikubo K. Affinity purification of recombinant cholera toxin B subunit oligomer expressed in Bacillus brevis for potential human use as a mucosal adjuvant. FEMS Immunol Med Microbiol 1998;20:311–318. [PubMed: 9626936]
26. Uesaka Y, Otsuka Y, Lin Z, et al. Simple method of purification of Escherichia coli heat-labile enterotoxin and cholera toxin using immobilized galactose. Microb Pathog 1994;16:71–76. [PubMed: 8057828]
27. Gray ES, Meyers T, Gray G, Montefiori DC, Morris L. Insensitivity of Paediatric HIV-1 Subtype C Viruses to Broadly Neutralising Monoclonal Antibodies Raised against Subtype B. PLoS Med 2006;3:e255. [PubMed: 16834457]
28. Li B, Decker JM, Johnson RW, et al. Evidence for potent autologous neutralizing antibody titers and compact envelopes in early infection with subtype C human immunodeficiency virus type 1. J Virol 2006;80:5211–5218. [PubMed: 16699001]
29. Binley JM, Wrin T, Korber B, et al. Comprehensive cross-clade neutralization analysis of a panel of anti-human immunodeficiency virus type 1 monoclonal antibodies. J Virol 2004;78:13232–13252. [PubMed: 15542675]

30. Zwick MB, Jensen R, Church S, et al. Anti-human immunodeficiency virus type 1 (HIV-1) antibodies 2F5 and 4E10 require surprisingly few crucial residues in the membrane-proximal external region of glycoprotein gp41 to neutralize HIV-1. J Virol 2005;79:1252–1261. [PubMed: 15613352]

31. Lenz O, Dittmar MT, Wagner A, et al. Trimeric membrane-anchored gp41 inhibits HIV membrane fusion. J Biol Chem 2005;280:4095–4101. [PubMed: 15574416]

32. Lu M, Blacklow SC, Kim PS. A trimeric structural domain of the HIV-1 transmembrane glycoprotein. Nat Struct Biol 1995;2:1075–1082. [PubMed: 8846219]

33. Mantis NJ, Kozlowski PA, Mielcarz DW, Weissenhorn W, Neutra MR. Immunization of mice with recombinant gp41 in a systemic prime/mucosal boost protocol induces HIV-1-specific serum IgG and secretory IgA antibodies. Vaccine 2001;19:3990–4001. [PubMed: 11427275]

34. Qiao ZS, Kim M, Reinhold B, Montefiori D, Wang JH, Reinherz EL. Design, expression, and immunogenicity of a soluble HIV trimeric envelope fragment adopting a prefusion gp41 configuration. J Biol Chem 2005;280:23138–23146. [PubMed: 15833740]

35. Schibli DJ, Montelaro RC, Vogel HJ. The membrane-proximal tryptophan-rich region of the HIV glycoprotein, gp41, forms a well-defined helix in dodecylphosphocholine micelles. Biochemistry (Mosc) 2001;40:9570–9578.

36. Tan K, Liu J, Wang J, Shen S, Lu M. Atomic structure of a thermostable subdomain of HIV-1 gp41. Proc Natl Acad Sci USA 1997;94:12303–12308. [PubMed: 9356444]

37. Trivedi VD, Cheng SF, Wu CW, Karthikeyan R, Chen CJ, Chang DK. The LLSGIV stretch of the N-terminal region of HIV-1 gp41 is critical for binding to a model peptide, T20. Protein Eng 2003;16:311–317. [PubMed: 12736375]

38. Viard M, Blumenthal R, Raviv Y. Improved separation of integral membrane proteins by continuous elution electrophoresis with simultaneous detergent exchange: application to the purification of the fusion protein of the human immunodeficiency virus type 1. Electrophoresis 2002;23:1659–1666. [PubMed: 12179985]

39. Weissenhorn W, Calder LJ, Dessen A, Laue T, Skehel JJ, Wiley DC. Assembly of a rod-shaped chimera of a trimeric GCN4 zipper and the HIV- 1 gp41 ectodomain expressed in Escherichia coli. Proc Natl Acad Sci USA 1997;94:6065–6069. [PubMed: 9177169]

40. Weissenhorn W, Dessen A, Harrison SC, Skehel JJ, Wiley DC. Atomic structure of the ectodomain from HIV-1 gp41. Nature 1997;387:426–430. [PubMed: 9163431]

41. Weissenhorn W, Wharton SA, Calder LJ, et al. The ectodomain of HIV-1 env subunit gp41 forms a soluble, alpha- helical, rod-like oligomer in the absence of gp120 and the N-terminal fusion peptide. EMBO J 1996;15:1507–1514. [PubMed: 8612573]

42. Wingfield PT, Stahl SJ, Kaufman J, et al. The extracellular domain of immunodeficiency virus gp41 protein: expression in Escherichia coli, purification, and crystallization. Protein Sci 1997;6:1653–1660. [PubMed: 9260278]

43. Santona A, Carta F, Fraghi P, Turrini F. Mapping antigenic sites of an immunodominant surface lipoprotein of Mycoplasma agalactiae, AvgC, with the use of synthetic peptides. Infect Immun 2002;70:171–176. [PubMed: 11748179]

44. Vanniasinkam T, Barton MD, Heuzenroeder MW. B-Cell epitope mapping of the VapA protein of Rhodococcus equi: implications for early detection of R. equi disease in foals J Clin Microbiol 2001;39:1633–1637.

45. Dakappagari NK, Pyles J, Parihar R, Carson WE, Young DC, Kaumaya PT. A chimeric multi-human epidermal growth factor receptor-2 B cell epitope peptide vaccine mediates superior antitumor responses. J Immunol 2003;170:4242–4253. [PubMed: 12682258]

46. Saez-Cirion A, Arrondo JL, Gomara MJ, et al. Structural and functional roles of HIV-1 gp41 pretransmembrane sequence segmentation. Biophys J 2003;85:3769–3780. [PubMed: 14645067]

47. Chen B, Vogan EM, Gong H, Skehel JJ, Wiley DC, Harrison SC. Structure of an unliganded simian immunodeficiency virus gp120 core. Nature 2005;433:834–841. [PubMed: 15729334]

48. Liljeqvist S, Ståhl S, Andréoni C, Binz H, Uhlén M, Murby M. Fusions to the cholera toxin B subunit: influence on pentamerization and GM1 binding. J Immunol Methods 1997;210:125–135. [PubMed: 9520296]

49. George-Chandy A, Eriksson K, Lebens M, Nordstrom I, Schon E, Holmgren J. Cholera toxin B subunit as a carrier molecule promotes antigen presentation and increases CD40 and CD86 expression on antigen-presenting cells. Infect Immun 2001;69:5716–5725. [PubMed: 11500448]
50. Bienenstock J, McDermott MR. Bronchus- and nasal-associated lymphoid tissues. Immunol Rev 2005;206:22–31. [PubMed: 16048540]
51. Alfsen A, Iniguez P, Bouguyon E, Bomsel M. Secretory IgA Specific for a Conserved Epitope on gp41 Envelope Glycoprotein Inhibits Epithelial Transcytosis of HIV-1. J Immunol 2001;166:6257–6265. [PubMed: 11342649]
52. Robinson WE Jr, Gorny MK, Xu JY, Mitchell WM, Zolla-Pazner S. Two immunodominant domains of gp41 bind antibodies which enhance human immunodeficiency virus type 1 infection *in vitro*. J Virol 1991;65:4169–4176. [PubMed: 2072448]
53. Finnegan CM, Berg W, Lewis GK, DeVico AL. Antigenic properties of the human immunodeficiency virus transmembrane glycoprotein during cell-cell fusion. J Virol 2002;76:12123–12134. [PubMed: 12414953]
54. Binley JM, Ditzel HJ, Barbas CF 3rd, et al. Human antibody responses to HIV type 1 glycoprotein 41 cloned in phage display libraries suggest three major epitopes are recognized and give evidence for conserved antibody motifs in antigen binding. AIDS Res Hum Retroviruses 1996;12:911–924. [PubMed: 8798976]
55. Tyler DS, Stanley SD, Zolla-Pazner S, et al. Identification of sites within gp41 that serve as targets for antibody-dependent cellular cytotoxicity by using human monoclonal antibodies. J Immunol 1990;145:3276–3282. [PubMed: 1700004]
56. Hessell AJ, Hangartner L, Hunter M, et al. Fc receptor but not complement binding is important in antibody protection against HIV. Nature 2007;449:101–104. [PubMed: 17805298]

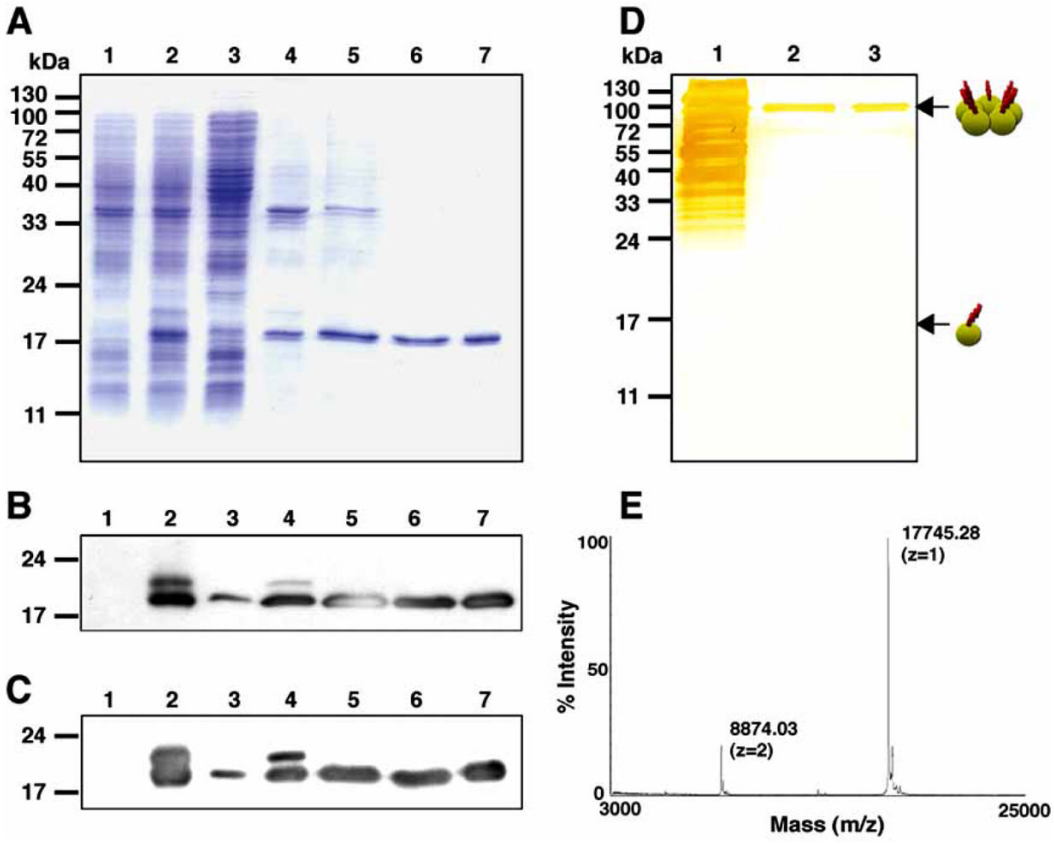

Fig. 1.

Expression and purification of CTB-MPR$_{649–684}$ in *E. coli*. *A:* SDS-PAGE analysis of CTB-MPR$_{649–684}$ purification steps. Lane 1: total *E. coli* proteins before induction; Lane 2: total *E. coli* proteins after induction; Lane 3: soluble fraction after cell disruption; Lane 4: insoluble fraction; Lane 5: CHAPS soluble fraction; Lane 6: cobalt affinity fraction; Lane 7: galactose affinity fraction. *B, C:* Same samples were analyzed by Western blotting using anti-CTB (B) and 2F5 (C). D: silver-stain of proteins resolved under a non-denaturing condition. Lane 1: CHAPS soluble fraction; Lane 2: cobalt affinity fraction; Lane 3: galactose affinity fraction. Arrows indicate the positions of monomer and pentamer of CTB-MPR$_{649–684}$. E: mass spectrometry analysis of purified CTB-MPR$_{649–684}$.

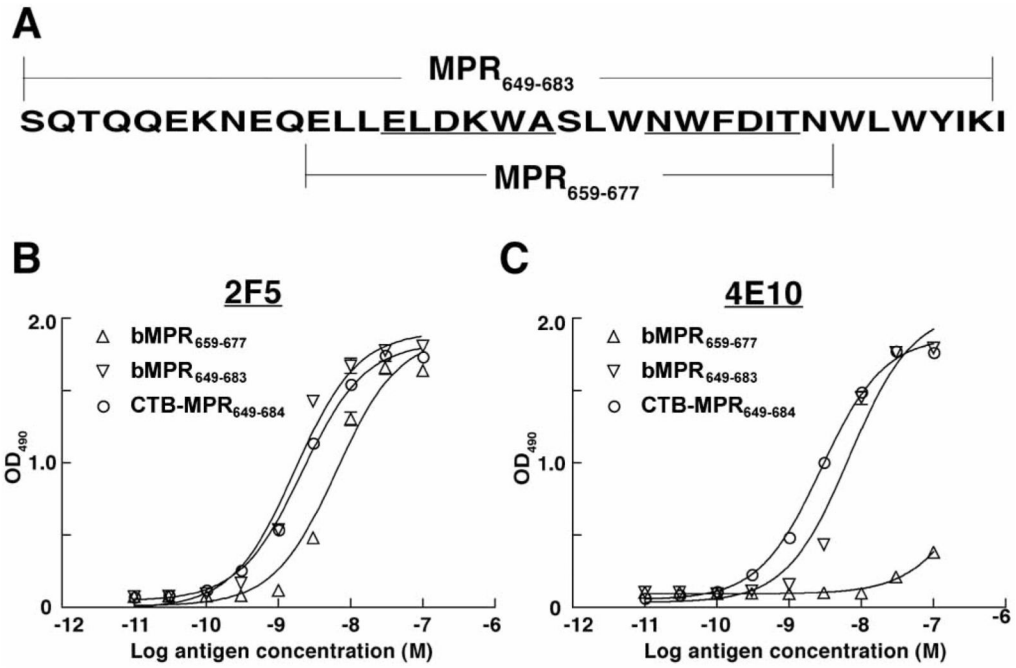

Fig. 2.

Analysis of mAbs 2F5 and 4E10 binding to MPR antigens. *A:* Schematic representation of $MPR_{649–683}$ and $MPR_{659–677}$ sequences. *B, C:* Binding of 2F5 (B) and 4E10 (C) to biotinylated $MPR_{659–677}$ ($bMPR_{659–677}$), biotinylated $MPR_{649–683}$ ($bMPR_{649–683}$) and CTB-$MPR_{649–684}$. Streptavidin (for the synthetic biotinylated MPR peptides) or GM1 ganglioside (for CTB fusion) were used to capture various concentrations of MPR antigens on plates, and 2F5 or 4E10 bound to the antigens were detected using HRP-conjugated anti-human secondary Abs and OPD substrate.

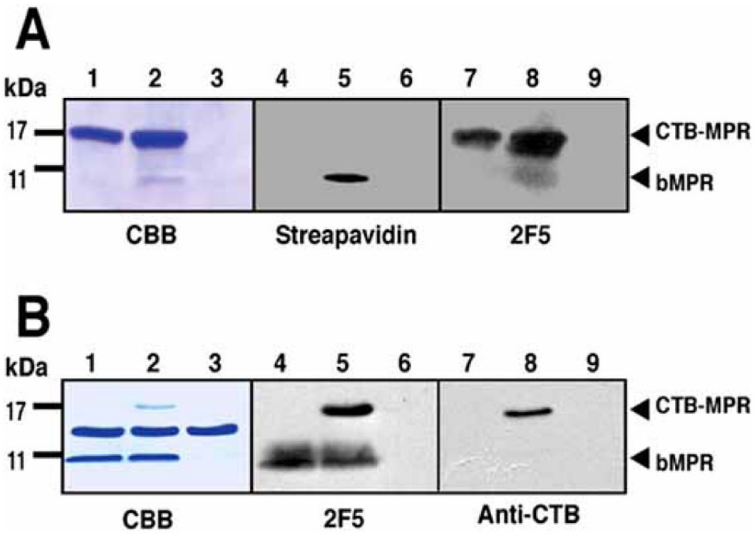

Fig. 3.

Analysis of specific association between the MPR domains of CTB-$MPR_{649–684}$ and biotinylated $MPR_{649–683}$ peptide. *A:* Co-precipitation assay. CHAPS-solubilized CTB-$MPR_{649–684}$ or native CTB (4 μM each) were mixed with the peptide, which were subsequently dialyzed to remove CHAPS. Precipitated fraction was analyzed by SDS-PAGE (lanes 1–3) and Western blotting (lanes 4–9) using streptavidin or 2F5. Lanes 1, 4, 7: CTB-$MPR_{649–684}$ alone, lanes 2, 5, 8: CTB-$MPR_{649–684}$ plus $bMPR_{649–683}$, lanes 3, 6, 9: CTB plus $bMPR_{649–683}$. *B:* Pull-down assay. CTB-$MPR_{649–684}$ or native CTB (0.6 μM each) in PBS, pH7.4 (without detergent) were incubated with $bMPR_{649–683}$. After capturing $bMPR_{649–683}$ with streptavidin-conjugated beads, bead-associated fraction was analyzed by SDS-PAGE and Western blotting using 2F5 or anti-CTB antiserum. Lanes 1, 4, 7: CTB plus $bMPR_{649–683}$, lanes 2, 5,8: CTB-$MPR_{649–684}$ plus $bMPR_{649–683}$, lanes 3, 6, 9: CTB-$MPR_{649–684}$ alone.

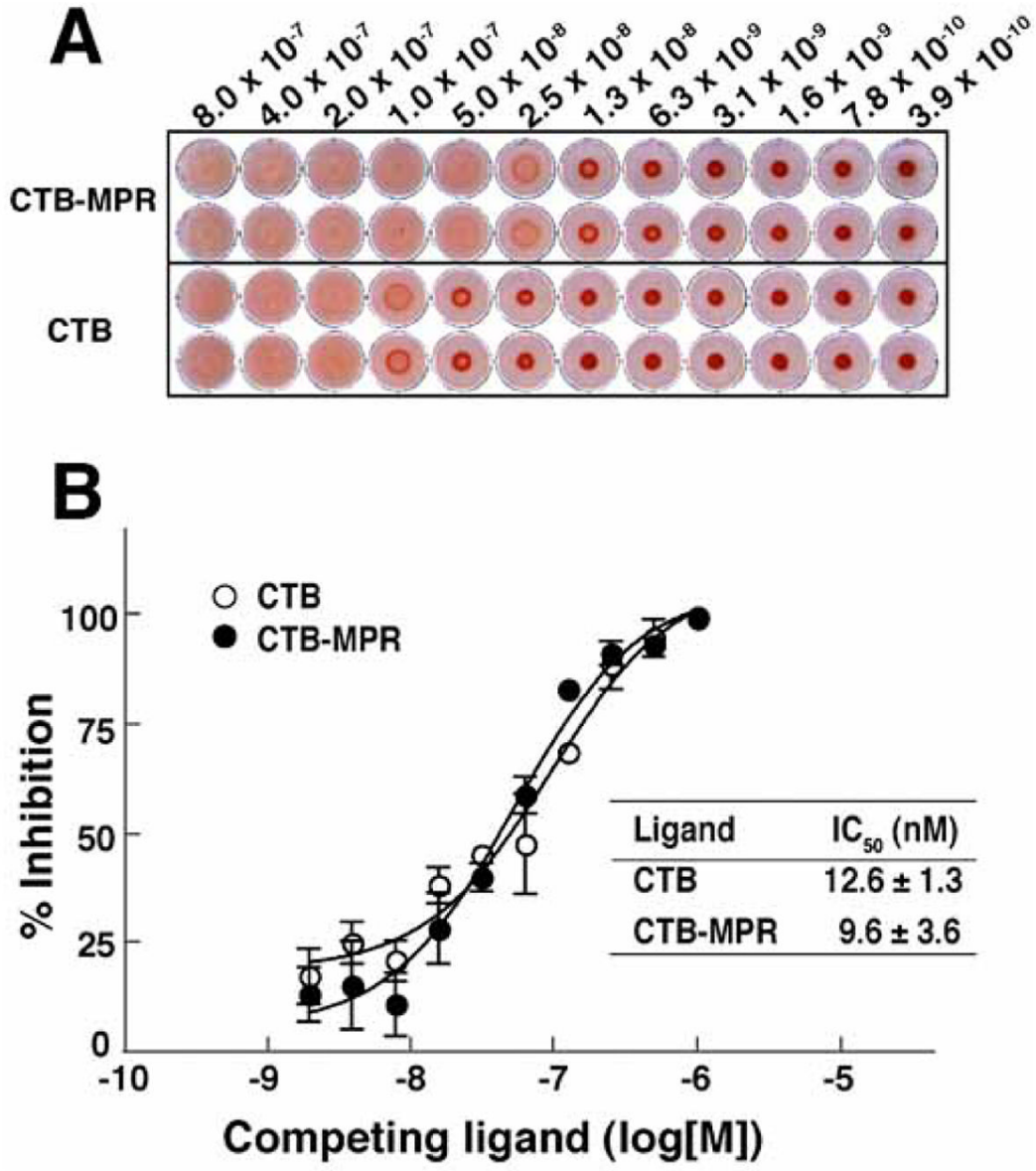

Fig. 4.

Comparison of affinities of CTB and CTB-MPR$_{649–684}$ to GM1 ganglioside. *A:* Hemagglutination assay using sheep red blood cells coated with GM1 ganglioside. Note that hemagglutinated cells are diffused whereas non-hemagglutinated cells sedimented in the wells. Samples were analyzed in duplicate. *B:* Competitive GM1-ELISA using biotinylated CTB. Biotinylated CTB was mixed with different concentrations of CTB or CTB-MPR$_{649–684}$, and amount of GM1-bound biotinylated CTB was determined with HRP-conjugated streptavidin. Inhibition constants (IC_{50}) were determined by non-linear regression analysis of data points at different concentrations of competitor using Prism software. Each data point represents mean ± S.E., n = 3.

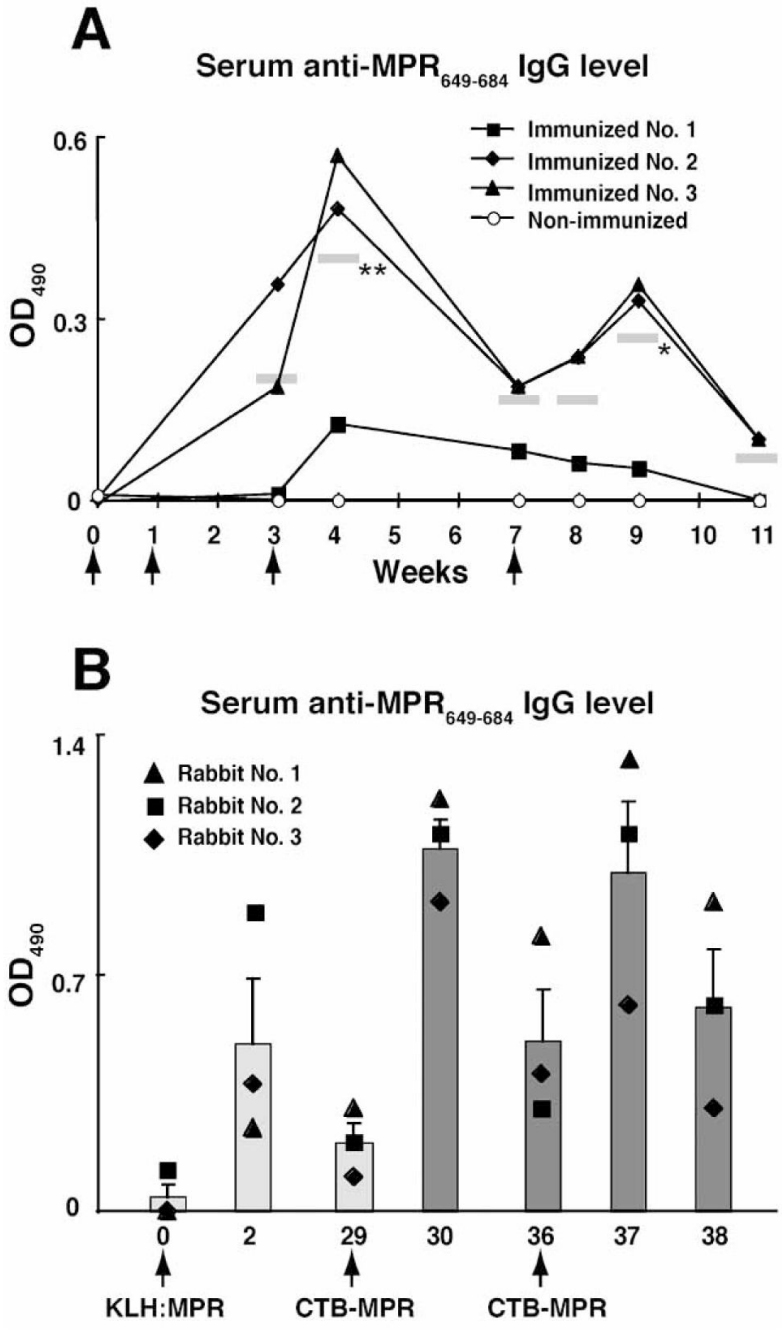

Fig. 5.

Immunization of rabbits with CTB-MPR$_{649–684}$. *A:* Serum anti-MPR IgG level of rabbits immunized with CTB-MPR$_{649–684}$. Twenty-five micrograms of the protein conjugated with liposome was subcutaneously given to rabbits at week 0, 1 and 3, and one hundred micrograms at week 7 (indicated with arrows). Endpoint titers (defined as reciprocal of the largest dilution giving OD>0.1 after subtracting the mean background value) were determined for Week 37, which are 1,600, 800, and 400 for rabbits 1–3, respectively. Horizontal bars in grey color represent the mean values of the three rabbits at each week time point. Asterisks next to the bars indicate statistical significance as compared to Week 0 (*$P < 0.05$, **$P < 0.01$). Statistical evaluation was performed by repeated-measures ANOVA with the Bonferroni's multiple

comparison test using the GraphPad Prism 4 software. *B:* Serum anti-MPR IgG level of rabbits immunized with KLH-conjugated with synthetic $MPR_{649–683}$ peptide (KLH:MPR) and CTB-$MPR_{649–684}$. Three rabbits were subcutaneously primed with 87.5 μg of KLH:MPR at week 0, and subsequently boosted with 25 μg of CTB-$MPR_{649–684}$ at week 29 and 36. Bars represent the average of the three immunized rabbits with S.E.M. Antibody levels of individual rabbits are also shown with symbols.

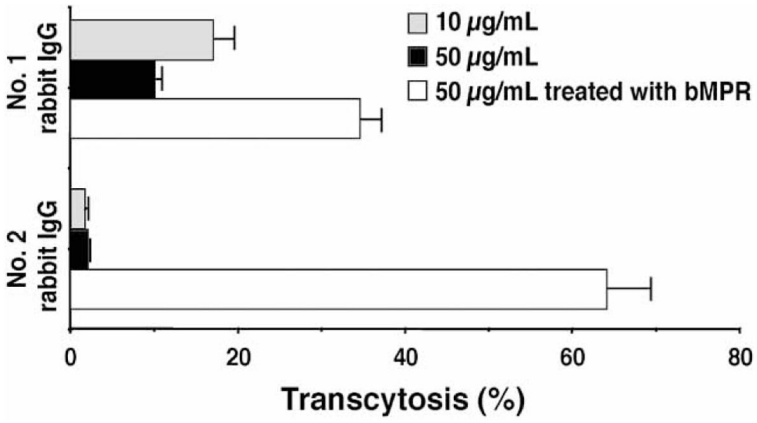

Fig. 6.

Transcytosis-blocking activity of rabbit serum anti-$MPR_{649–683}$ IgGs. IgG samples at 10 and 50 μg/mL, or 50 μg/mL samples pre-treated with biotinylated $MPR_{649–683}$ peptide were analyzed for transcytosis-blocking activity. IgG samples were purified from two highly responding rabbits (No. 1 and 2 rabbits in Fig. 5B) immunized with KLH:MPR and CTB-$MPR_{649–684}$ using Protein A beads. Percent transcytosis activity (mean ± SEM) was calculated by comparing to the rate of transcytosis obtained with an IgG sample from untreated rabbit (mean ± SEM).

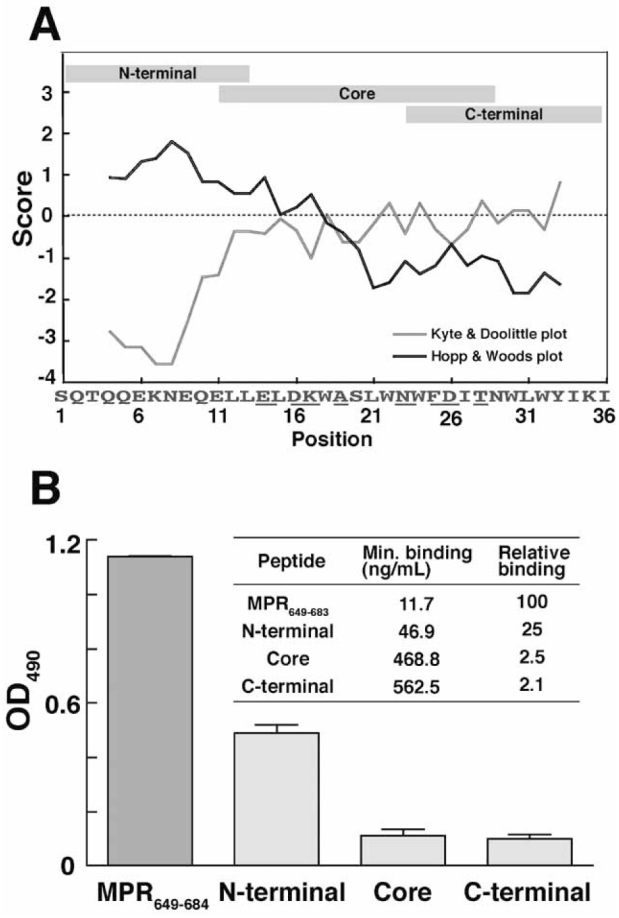

Peptide	Min. binding (ng/mL)	Relative binding
$MPR_{649-683}$	11.7	100
N-terminal	46.9	25
Core	468.8	2.5
C-terminal	562.5	2.1

Fig. 7.

Antigen-binding profile of anti-$MPR_{649–683}$ IgGs. *A:* Schematic representation of fragment MPR peptides used for epitope mapping. Hydropathy analysis based on Hopp & Woods plot (black line) and Kyte & Doolittle plot (gray line) of $MPR_{649–684}$ sequence is also shown. The average values of each seven-amino acid fragment of $MPR_{649–684}$ are plotted along the sequence. *B:* Epitope mapping anti-$MPR_{649–684}$ IgGs. Binding of anti-$MPR_{649–683}$ IgGs to different MPR peptides were analyzed by ELISA. One micromolar of the biotin-labeled peptides were captured with streptavidin coated on ELISA plates, which were incubated with 0.75 μg/mL of IgGs. Average values of the two IgG samples used in transcytosis assay, analyzed in duplicate, are shown with standard error. The embedded table shows the average of minimal detectable concentrations of IgG samples binding to each MPR peptide, and relative binding activity of IgG samples to fragment MPR peptides comparing with that to $MPR_{649–683}$.

Table 1

Apparent Affinities of 2F5 and 4E10 to MPR Antigens

Antigen	*K*d (nM)[1]	
	2F5	4E10
CTB-MPR$_{649–684}$	2.0	2.6
bMPR$_{649–683}$	1.7	6.9
bMPR$_{659–677}$	5.5	44.3

[1]Binding constants (*K*d) were determined by non-linear regression analysis of specific binding using Prism software. bMPR: biotinylated MPR.

Table 2

Clade B Pseudovirus Neutralization Assay of Rabbit IgG in TZM-bl Cells[1]

Sample[2]	ID50[3]				
	MN	**SF162.LS**	**WITO4160.33**	**REJO4541.67**	**SC422661.8**
Rabbit No 1	>60 μg/mL	>60 μg/mL	>60 μg/mL	>60 μg/mL	>60 μg/mL
Rabbit No 2	>110 μg/mL	>110 μg/mL	>110 μg/mL	>110 μg/mL	>110 μg/mL
untreated control	>45 μg/mL	>45 μg/mL	>45 μg/mL	>45 μg/mL	>45 μg/mL

[1] TZM-bl cells were incubated for 48 h at 37°C with two hundred $TCID_{50}$ of pseudovirus premixed with purified IgG samples. Luciferase activity of cell lysate was measured to determine the viral infectivity.

[2] IgG samples were purified from the corresponding number of rabbits in Fig. 5B or from an untreated control rabbit.

[3] ID50 was defined as the sample concentration giving 50 percent reduction in relative luminescence units compared to no-sample virus controls. Details are described in Materials and Methods. The Env-pseudotyped viruses were selected because they are highly sensitive to neutralization by 2F5 and 4E10 [19].

Table 3

SF162 Neutralization Assay of Rabbit IgG in Human PBMC[1]

Sample[2]	ID50[3]
Rabbit No 1	>120 μg/mL
Rabbit No 2	>220 μg/mL
Untreated control	>90 μg/mL
HIV-1-neutralizing human plasma	1:658 dilution

[1] Phytohemagglutinin-stimulated PBMCs were incubated for 72 h at 37°C with 100 $TCID_{50}$ HIV-1 premixed with each sample. After culturing in fresh medium for additional 24 h, viral expression was assayed by determining p24 levels.

[2] IgG samples were purified from the corresponding number of rabbits in Fig. 5B or from an untreated control rabbit.

[3] ID50 was defined as sample concentration (for IgG samples) or dilution (for human plasma positive control) that gave 50 percent reduction in the amount of p24 detected from no-sample virus controls. Details are described in Materials and Methods.